Ceramics International 46 (2020) 15236–15241

Contents lists available at ScienceDirect

Ceramics International

journal homepage: www.elsevier.com/locate/ceramint

# Enhancement of Urbach's energy and non-lattice oxygen content of $TiO_{1.7}$ ultra-thin films for more photocatalytic activity

Mai S.A. Hussien[a], S.S. Shenouda[b,*], B. Parditka[c], A. Csík[d], Z. Erdélyi[c]

[a] Chemistry Department and Nanoscience laboratory for environmental and biomedical applications, Faculty of Education, Ain Shams University, Roxy, Cairo, Egypt
[b] Physics Department, Faculty of Education, Ain Shams University, Roxy, Cairo, Egypt
[c] Department of Solid State Physics, Faculty of Science and Technology, University of Debrecen, P.O. Box 400, H-4002, Debrecen, Hungary
[d] Institute for Nuclear Research, Debrecen, Hungary

ARTICLE INFO

*Keywords:*
Amorphous $TiO_{1.7}$
Ultra-thin film
Urbach's energy
Non-lattice oxygen
Photocatalysis

ABSTRACT

This research presents strong photocatalytic activity for amorphous $TiO_{1.7}$ prepared by atomic layer deposition to decompose the LBR (Levafix Brilliant Red) dye. LBR is an example of the pollutant dyes in the textile industrial wastewater. This activity has been enhanced significantly through decreasing the thickness from 40 to 8 nm. This behavior is explained by correlating the photocatalytic, optical, structural and photoluminescence properties. The thinner film has higher Urbach's energy (wider tail of localized states) and higher life time of the photo-generated charge carriers. This is attributed to increasing the non-lattice oxygen content which enhances the photocatalytic behavior of thinner films. Moreover, these ultra-thin films have ability to be recycled by the same efficiency indicating its promising application in the water purification from the organic dyes and pollutants.

## 1. Introduction

Recently, photocatalysis has attracted much attention as a potential method for water treatment by decomposition of the wastes and toxic organic dyes [1–4]. This could be achieved by the facile formation of radicals through the UV irradiation of the photocatalyst (wide band gap semiconductor with strong oxidative ability) [4,5]. The photo-generated electrons and holes react with the oxygen molecules and hydroxyl groups on the catalyst's surface, producing super-oxide radical ions and hydroxyl radicals, respectively [2,4].

Titanium dioxide ($TiO_2$) is one of the promising photocatalysts due to its high activity for degradation of organic compounds and dyes, high chemical stability, low cost, nontoxicity, strong oxidizing power, low quantum efficiency of photocatalytic reactions, wide availability, high refractive index and chemical inertness [1,6–10]. Disadvantages of the heterogeneous photocatalysis such as the stirring during the reaction to avoid agglomeration of $TiO_2$ particles could be reduced using $TiO_2$ thin films [4,10].

Oxygen vacancies as point defects play an important role in photocatalytic reaction by formation of defect states below the conduction band [11]. In this research, these vacancies could be developed by preparing non-stoichiometric ($TiO_{1.7}$) thin films using plasma enhanced atomic layer deposition. These films show strong photocatalysis for the LBR dye. Further vacancies and more photocatalytic activity could be achieved through decreasing the film thickness. This increased content of the oxygen vacancies has been detected through the non-lattice oxygen on the XPS spectra. Enhancement of the photocatalytic activity has been explained by correlating the structural, optical and photoluminescence properties. Enhancement of the photocatalysis by means of decreasing the film thickness agrees with that of Al-rich:$Al_2O_3$ attributed to increasing the Al content which decreases the energy gap [12]. Furthermore, $TiO_{1.7}$ has more photocatalytic activity than Al-rich:$Al_2O_3$ with the same film thickness.

## 2. Methods and structure identification

Different thicknesses of $TiO_{1.7}$ (8, 15, 25 and 40 nm) have been grown on different substrates by atomic layer deposition ALD (Beneq TFS 200) in plasma-enhanced mode with RF power 50 W at 50 °C. During the deposition, the pressure inside the reactor and chamber was 1.2 and 7.4 mbar, respectively. The ALD cycle was as following: 200 ms $TiCl_4$ followed by 3s purge, then 3s of oxygen plasma and another 3s purge. The thickness of the films has been measured using an AMBIOS XP-1 profilometer. In order to confirm the film thickness, TEM-lamella of the films has also been prepared by focused ion beam (FIB) and the thickness was checked by the electron microscope (Thermo Scientific

* Corresponding author.
*E-mail address:* shenouda.fam@edu.asu.edu.eg (S.S. Shenouda).

https://doi.org/10.1016/j.ceramint.2020.03.062
Received 20 January 2020; Received in revised form 27 February 2020; Accepted 5 March 2020
Available online 08 March 2020

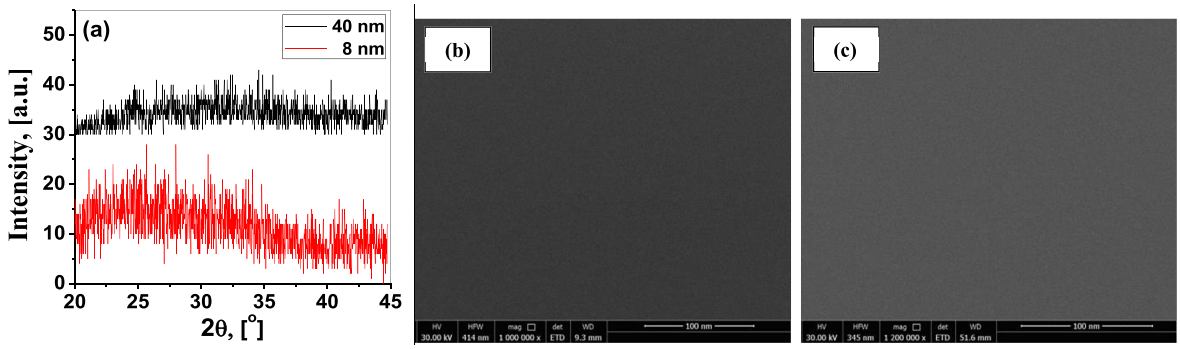


**Fig. 1.** (a) XRD of $TiO_{1.7}$ (40 and 8 nm); (b) HR-SEM of $TiO_{1.7}$ (40 nm); (c) HR-SEM of $TiO_{1.7}$ (8 nm).

Scios 2 Dual Beam FIB + SEM).

X-ray diffraction (XRD) of the films (8 and 40 nm) was measured by Philips X-ray diffractometer (PAN analytical X'Pert PRO) utilizing Cu $K_\alpha$ monochromatic radiation (40 kV, 40 mA). Fig. 1(a) shows the absence of peaks in the XRD indicating the amorphous structure of the prepared films. Also, the amorphous structure has been confirmed using high resolution scanning electron microscope (HR-SEM, QUANTA FEG 250, USA) as shown in Fig. 1(b and c).

For further structure identification and elemental analysis, X-ray Photoelectron spectroscopy (XPS) spectra were obtained by X-ray irradiation using an Al $K_\alpha$ source (10 mA, 10 kV). The photoelectrons were detected by the hemispherical energy analyzer (type PHOIBOS-100, SPECS GmbH, Berlin). The ultimate vacuum was $5x10^{-10}$ mbar. The used reference peak is C 1s with binding energy of 284.5 eV. The peaks were identified using NIST XPS Database [13]. Fig. 2(a and b) shows the XPS spectra of 40 and 8 nm films as examples. For characterization of chemical state, the O 1s, C 1s and Ti 2p peaks were measured with 10 eV pass energy. CasaXPS software was applied in the deconvolution and fitting procedure to determine the elemental composition and lattice/nonlattice oxygen content. The composition of Ti and O are 37% and 63%, respectively, for all samples with different thicknesses. These show that our films are $TiO_{1.7}$, i.e. not stoichiometric $TiO_2$ but Ti-rich.

For the photocatalysis investigations, UV lamp of wavelength (254 nm) is used in an in-situ photo-reactor (see its schematic in [12]). All thin film samples have area 3.125 $cm^2$. They were submerged flatly at the bottom of the dye container at distance 5 cm below the lamp. Different concentrations of the LBR dye were checked and the $10^{-4}$ M concentration has been chosen for the detailed investigations.

Adsorption of the dye over the $TiO_{1.7}$ films with different thicknesses has been determined before the photocatalysis reaching to the equilibrium before 30 min. The adsorption has a Langmuir-type balance according the equation [14]:

$$\theta = \frac{Q_e}{Q_{max}} = \frac{k_{ads} C_e}{1 + k_{ads} C_e} \quad (1)$$

Where $\theta$ is coverage, $Q_e$ is the quantity of adsorbed molecules at the adsorption equilibrium, $Q_{max}$ is maximum adsorbed quantity, $k_{ads}$ is Langmuir adsorption constant of LBR and $C_e$ is the concentration of LBR at the adsorption equilibrium. Eq. (1) can be expressed as:

$$\frac{1}{Q_e} = \frac{1}{Q_{max}} + \frac{1}{Q_{max} k_{ads} C_e} \quad (2)$$

Fig. 3 confirms the linear relation between $\frac{1}{Q_e}$ and $\frac{1}{C_e}$. Values of $k_{ads}$ for each thickness have been determined ($k_{ads} = intersept/slope$) and listed in Table 1. The value of $k_{ads}$ (0.06 ± 0.01 L/mmol) is considered significantly smaller than that reported in literature for materials used to remove the same dye from water by adsorption such as H-type activated carbon ($k_{ads}$ = 23 L/mmol ) [14].

Transmittance of the films deposited on Quartz substrates was measured by unpolarized light in the wavelength range 190–2500 nm at normal incidence and room temperature using JASCO double beam spectrophotometer (V-670, JAPAN). The baseline has been sited using similar quartz substrates. The photoluminescence life time data were determined using a 'PerkinElmer LS55 USA' Luminescence Spectrometer with excitation wavelength 325 nm.

## 3. Results and discussion

The photocatalytic degradation of the LBR dye ($\frac{C}{C_o}$ versus time) using different thicknesses of $TiO_{1.7}$ thin film (40, 25, 15 and 8 nm) is shown in Fig. 4(a). $C_o$ and $C$ are the initial and current concentrations of the dye (mg/L), respectively. Clearly, these thin films have strong and fast photocatalytic degradation obeying the first order reaction equation [12,15,16] as shown in Fig. 4(b):

$$\ln \frac{C}{C_o} = -kt \quad (3)$$

where $t$ is the illumination time, and $k$ is the apparent reaction rate constant. The values of $k$ were determined from the best fitting and presented in Table 2.

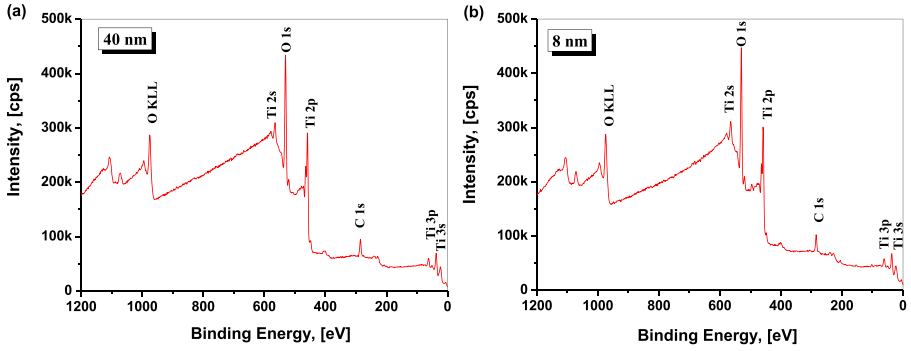


**Fig. 2.** XPS spectra of $TiO_{1.7}$ films with a thickness of: (a) 40 nm; (b) 8 nm.

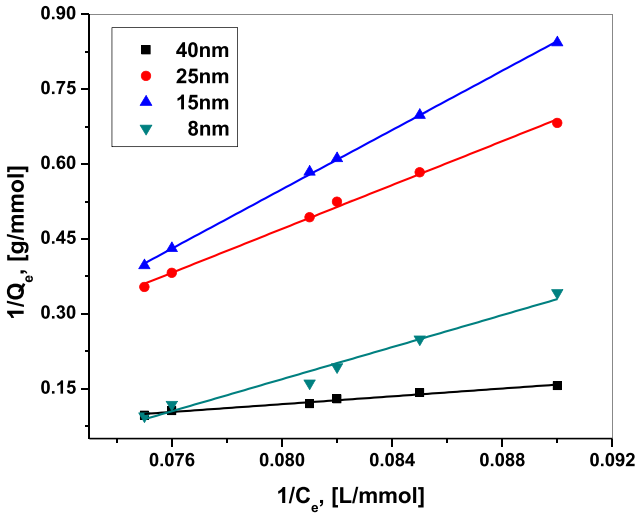


**Fig. 3.** Adsorption curves of LBR over $TiO_{1.7}$ with different thicknesses.

**Table 1**
Adsorption constant for LBR dye over $TiO_{1.7}$ with different thicknesses.

| Thickness, [nm] | $k_{ads}$, [L/mmol] |
|---|---|
| 40 | 0.050 |
| 25 | 0.059 |
| 15 | 0.061 |
| 8 | 0.069 |

Clearly, the rate of degradation increases with decreasing the film thickness. The amorphous $TiO_{1.7}$ (8 nm) ultra-thin film could achieve completion of degradation (about 100%) after 30 min. This degradation is faster than that achieved by the pure rutile $TiO_2$ (degradation rate 20% of Methyl orange after 30 min with sample's area 1 $cm^2$ as shown in Fig. 8 in ref. [1]) and the anatase $TiO_2$ (degradation rate 30% of Methylene blue after 30 min as shown in Fig. 9 in ref. [10] with $k = 0.015\ min^{-1}$). Also, it is faster than Al-rich:$Al_2O_3$(8 nm) which has $k = 0.115$ for LBR [12]. For further investigations, $TiO_{1.7}$ (8 nm) was recycled to degrade the dye with the same initial concentration as shown in Fig. 4(c). It is clear that this ultra-thin film works with the same strong rate for the five times. This means that fast water treatment could be achieved with lower cost, effort and time using ultra-thin amorphous $TiO_{1.7}$ film.

This strong photocatalytic degradation of dyes using $TiO_{1.7}$ could be explained as following: if $TiO_{1.7}$ is exposed to photon radiation $h\upsilon$ (≥ the energy gap, Eg ), electron of the valence band will be transited into the conduction band leaving hole in the valence band leading to formation of electron-hole pair [15]. These photo-generated electrons and holes could diffuse to the $TiO_{1.7}$ surface to react with $H_2O$, $O_2$ and OH- on the surface and produce hydroxyl radicals ($OH^{\bullet}$), superoxide radicals ($O_2^{\bullet}$) and $H_2O_2$. These radicals are able to decompose the organic materials [15]. Vacancies of the non-stoichiometric $TiO_{1.7}$ work as defect states in the energy gap to enhance the photocatalysis activity.

To understand this enhanced behavior of the thinner films, the optical properties have been investigated. The transmittance $T$ of the films is presented in Fig. 5(a) showing high transparency over a wide range of wavelengths which decreases suddenly in the UV region. The absorption coefficient $\alpha$ was calculated using Beer-Lambert's law [12,17]:

$$\alpha = \frac{1}{d}\ln\frac{1}{T} \tag{4}$$

where $d$ is the film thickness. The wavelength dependence of $\alpha$ is shown in Fig. 5(b). Clearly, the absorption coefficient peak shifts to higher wavelength (less photon energy) with decreasing the thickness.

The region of high absorption coefficient was analyzed by the following relation [18–20]:

$$\alpha h\upsilon = constant\,(h\upsilon - E_g)^m \tag{5}$$

The exponent $m$ determines the type of the optical transition since it has values 0.5 and 2 in case of direct and indirect allowed transitions, respectively. Fig. 6(a) shows that the films have indirect allowed transition with energy gap about 3.2 and 3.1 eV for the 40 and 8 nm films, respectively. The values of the energy gaps are less than that reported for thicker amorphous $TiO_2$ films by Hanini et al. [21] and Guang-lei et al. [22] ($E_g$ = 3.42 eV for 170 nm prepared by sol-gel technique [22] and $E_g$ = 3.38 eV for 500 nm prepared by conventional electron beam evaporation deposition [22]). Also, the obtained values of $E_g$ are less than the used UV radiation. This enables the films to work as strong photocatalysts.

The region of low absorption coefficient was found to obey Urbach's rule [18]:

$$\alpha = constant\,\exp\left(\frac{h\upsilon}{E_e}\right) \tag{6}$$

where $E_e$ is Urbach's energy measuring the tail width of localized states in the band gap of the amorphous semiconductors representing the degree of disorder [18]. Values of $E_e$ were estimated from the linear relation between $\ln\alpha$ and $h\upsilon$ (see Fig. 6(b)) and presented in Table 2. Clearly, Urbach's energy increases with decreasing the thickness (i.e. the degree of disorder in the film's structure increases).

Borrego Pérez et al. [23]. and Divya et al. [24]. could enhance the photocatalysis with increasing the Urbach energy in $TiO_2$ and ZnO, respectively. This increase in $E_e$ was achieved by doping and illustrated as extensions of localized states, generating defects or impurity energy levels in the energy bands [23,25,26]. The high $E_e$ is associated with existence of large number of oxygen vacancies. This leads to higher separation of photo-generated carriers improving the photocatalysis behavior [23,27]. Here, increasing of the Urbach's energy could be achieved simply by decreasing the thickness of the amorphous $TiO_{1.7}$ film instead of doping.

With further consideration of the XPS, the peak (O 1s) could be fitted into 2 peaks corresponding to lattice oxygen (LO) and non-lattice

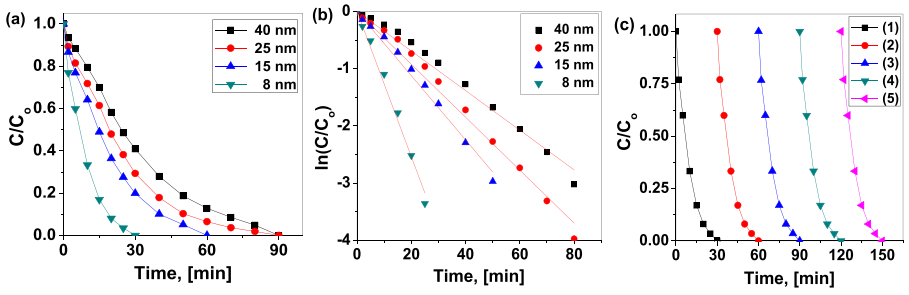


**Fig. 4.** (a) Photocatalytic degradation of LBR dye using different thicknesses of $TiO_{1.7}$; (b) $\ln\frac{C}{C_o}$ versus time; (c) Recycling test of $TiO_{1.7}$(8 nm).

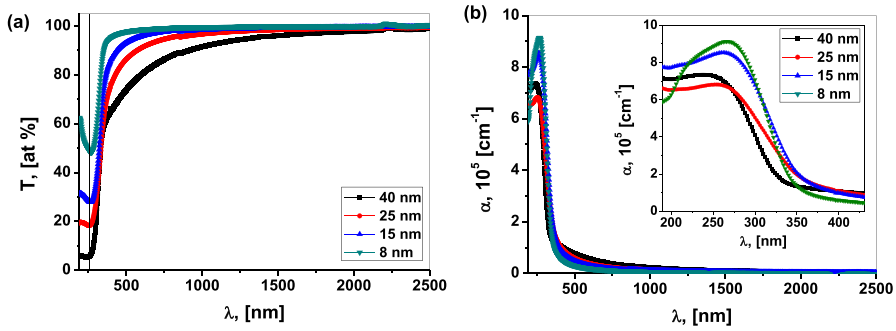


**Fig. 5.** (a) Transmittance spectra of $TiO_{1.7}$(40 - 8 nm) thin films; (b) wavelength dependence of the absorption coefficient.

oxygen (NLO). LO corresponds to the stoichiometric $TiO_2$ while NLO corresponds to the non-stoichiometric $TiO_{2-x}$ and proportional to the number of oxygen vacancies [28]. Fig. 7(a and b) shows that the thinner film (8 nm) has more NLO than the thicker film (40 nm) in the most upper layer detected by the XPS. Although, both thicknesses have similar composition representing similar percentage of O compared to Ti, the thinner film has more oxygen vacancies developed as oxygen left from their regular lattice position. This excess of oxygen vacancies illustrates the increase of Urbach's energy and tail's width of the localized states of the thinnest film (8 nm). This contributes to higher separation of charge carriers, decreases the recombination of charge carriers and increases their life time to reach to the surface and participate in the photocatalysis process. This enhances the photocatalysis behavior [23,24,26].

For further interpretation, the photolumenscence PL life time ($\tau$) and recombination rate ($r = 1/\tau$) were determined for the $TiO_{1.7}$ films from the normalized PL decay curves (see Fig. 8). The normalized intensity $I/I_o$ could be fitted by an exponential function: $I/I_o = \exp\left(\frac{-t}{\tau}\right)$ where $I_o$ is the initial intensity [29]. The life time increased from 0.104 ms to 0.144 ms while the recombination rate decreased from 9.6 $ms^{-1}$ to 6.9 $ms^{-1}$ with decreasing the film thickness from 40 to 8 nm. This results from the wider tail of the thinner film. Thus, the photo-generated charge carriers in the thinner film have higher chance to reach to the film surface and participate in the photocatalysis process.

## 4. Conclusion

We have successfully enhanced the photocatalytic behavior of $TiO_{1.7}$ thin films for water purification from Levafix Brilliant Red dye as example of organic pollutants. This enhancement could be achieved with decreasing the film thickness. These ultra-thin films have been prepared using ALD with plasma mode. The higher photocatalytic activity of the thinner film is attributed to: wider tail of localized states (0.66 eV) resulting from its higher disorder and more non-lattice oxygen content (30%); higher life time and lower recombination rate of the photo-generated charge carriers. These ultra-thin films could be recycled as photocatalyst for many times with the same efficiency.

## CRediT authorship contribution statement

**Mai S.A. Hussien:** Methodology, Investigation, Formal analysis, Writing - original draft. **S.S. Shenouda:** Conceptualization, Methodology, Investigation, Formal analysis, Writing - original draft. **B. Parditka:** Methodology, Writing - original draft. **A. Csík:** Investigation, Formal analysis. **Z. Erdélyi:** Supervision, Conceptualization, Formal analysis, Writing - review & editing.

## Declaration of competing interest

The authors declare that they have no conflict of interests.

## Acknowledgment

This research was funded by the Ministry of Higher Education and Scientific Research in Egypt (missions sector). Also, it was financed by the Higher Education Institutional Excellence Program (NKFIH-1150-6/2019) of the Ministry of Innovation and Technology in Hungary, in the framework of the Energetics thematic program of the University of Debrecen. The work was also supported by the International Relations office at University of Debrecen (coordinated by Mr. Péter Gara) through the Erasmus Credit Mobility program. Authors are acknowledging the GINOP-2.3.2-15-2016-00041 project, which is co-financed by the European Union and the European Regional Development Fund.

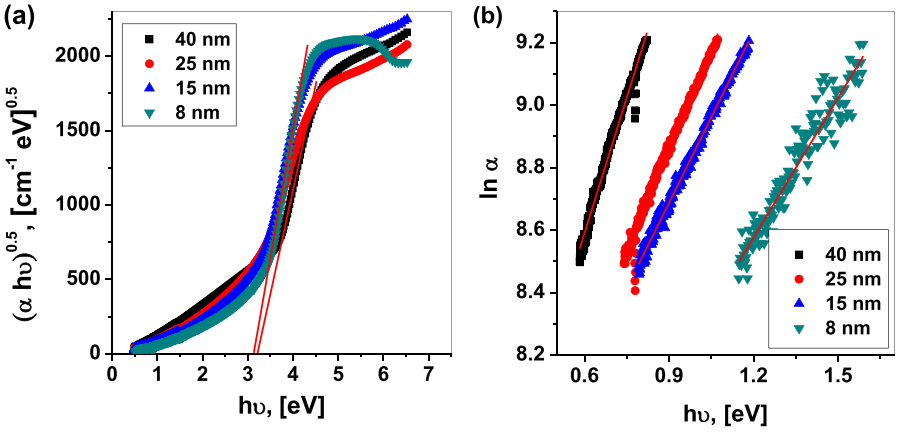


**Fig. 6.** (a) $(\alpha h\upsilon)^{1/2}$ versus $h\upsilon$, (b) $(\ln \alpha)$ versus $h\upsilon$.

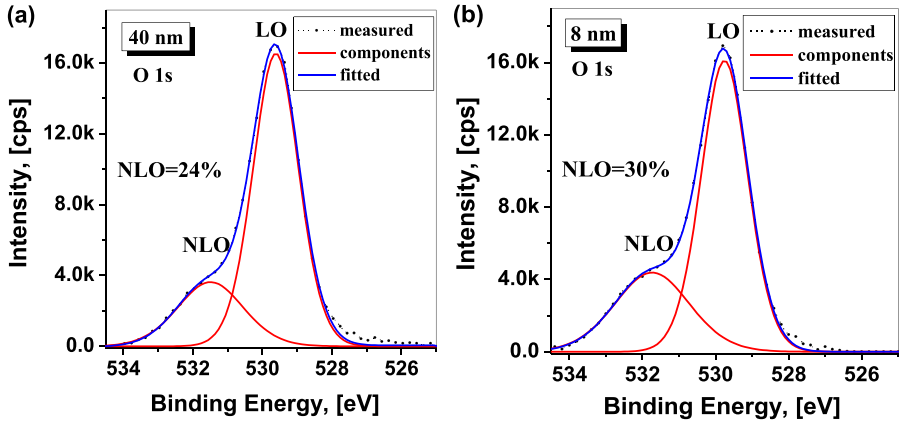


**Fig. 7.** O1s peaks of $TiO_{1.7}$ fitted into 2 peaks corresponding to lattice oxygen (LO) and non-lattice oxygen (NLO): (a) 40 nm; (b) 8 nm.

**Table 2**
Values of the apparent reaction rate constant (k) and Urbach's energy ($E_e$).

| Thickness, [nm] | $k$, $[min^{-1}]$ | $E_e$, $[eV]$ |
|---|---|---|
| 40 | 0.04 | 0.35 |
| 25 | 0.05 | 0.46 |
| 15 | 0.06 | 0.54 |
| 8 | 0.13 | 0.66 |

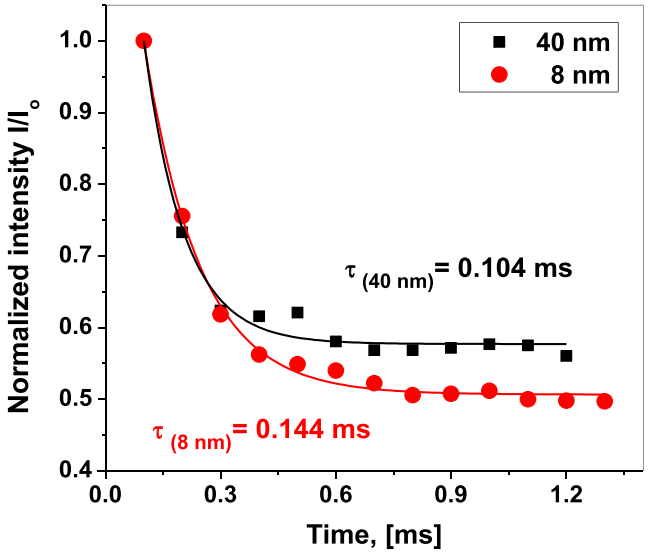


**Fig. 8.** Normalized photoluminescence decay of $TiO_{1.7}$ thin films (40 and 8 nm).

The authors would like to thank Prof. Mona Saif (Ain Shams University) for measuring the photoluminescence decay of the films and Dr. Csaba Cserháti (University of Debrecen) for measuring the film thickness utilizing SEM + FIB.

## References

[1] J. Tao, Z. Gong, G. Yao, Y. Cheng, M. Zhang, J. Lv, S. Shi, G. He, X. Jiang, X. Chen, Z. Sun, Enhanced optical and photocatalytic properties of Ag quantum dots-sensitized nanostructured TiO2/ZnO heterojunctions, J. Alloys Compd. 688 (2016) 605.
[2] C.H.A. Tsang, H.Y.H. Kwok, Z. Cheng, D.Y.C. Leung, The applications of graphene-based materials in pollutant control and disinfection, Prog. Solid State Chem. 45–46 (2017) 1.
[3] M.A. Brown, S.C. De Vito, Predicting azo dye toxicity, Crit. Rev. Environ. Sci. Technol. 23 (1993) 249.
[4] S. Watson, D. Beydoun, J. Scott, R. Amal, Preparation of nanosized crystalline $TiO_2$ particles at low temperature for photocatalysis, J. Nano Res. 6 (2004) 193.
[5] R. Ghosh, Rakesh P. Sahu, Ranjan Ganguly, Igor Zhitomirsky, Ishwar K. Puria, Photocatalytic activity of electrophoretically deposited TiO2 and ZnO nanoparticles on fog harvesting meshes, Ceram. Int. 46 (2020) 3777–3785.
[6] J. Singh, K. Sahu, S. Choudhary, A. Bisht, S. Mohapatra, Thermal annealing induced cave in and formation of nanoscale pits in Ag–TiO2 plasmonic nanocomposite thin film, Ceram. Int. 46 (2020) 3275–3281.
[7] Y. Li, S. Cao, A. Zhang, C. Zhang, T. Qu, Y. Zhao, A. Chen, Carbon and nitrogen co-doped bowl-like Au/$TiO_2$ nanostructures with tunable size for enhanced visible-light-driven photocatalysis, Appl. Surf. Sci. 445 (2018) 350–358.
[8] Z. Duan, Y. Zhu, P. Ren, J. Jia, Shu Yang, G. Zhao, Y. Xie, J. Zhang, Non-UV activated superhydrophilicity of patterned Fe-doped TiO2 film for anti-fogging and photocatalysis, Appl. Surf. Sci. 452 (2018) 165–173.
[9] M. Danish, S. Ambreen, A. Chauhan, A. Pandey, Optimization and comparative evaluation of optical and photocatalytic properties of TiO2 thin films prepared via sol–gel method, J. Saudi Chem. Soc. 19 (2015) 557.
[10] F. Bensouici, M. Bououdina, A.A. Dakhel, R. Tala-Ighil, M. Tounane, A. Iratni, T. Souier, S. Liu, W. Cai, Optical, structural and photocatalysis properties of Cu-doped TiO2 thin films, Appl. Surf. Sci. 395 (2017) 110.
[11] S. Kim, K.C. Ko, J.Y. Lee, F. Illas, Single oxygen vacancies of $(TiO_2)_{35}$ as a prototype of reduced nanoparticle: implication to photocatalytic activity, Phys. Chem. Chem. Phys. 18 (2016) 23755–23762.
[12] S.S. Shenouda, Mai S.A. Hussien, B. Parditka, A. Csík, V. Takats, Z. Erdélyi, Novel amorphous Al-rich $Al_2O_3$ ultra-thin films as active photocatalysts for water treatment from some textile dyes, Ceram. Int. 46 (2020) 7922–7929.
[13] https://srdata.nist.gov/xps/.
[14] M.I. El-Barghouthi, A.H. El-Sheikh, Y.S. Al-Degs, M. Gavin, WalkerAdsorption behavior of anionic reactive dyes on H-type Activated carbon: competitive adsorption and desorption studies, Separ. Sci. Technol. 42 (2007) 2195–2220.
[15] L. Wu, H. Yan, X. Li, X. Wang, Characterization and photocatalytic properties of $SnO_2$–$TiO_2$ nanocomposites prepared through gaseous detonation method, Ceram. Int. 43 (2016) 907.
[16] Chi Hieu Nguyen, Mai Lien Tran, Thi Tuong Van Tran, Ruey-Shin Juang, Enhanced removal of various dyes from aqueous solutions by UV and simulated solar photocatalysis over $TiO_2$/ZnO/rGO composites, Separ. Purif. Technol. 232 (2020) 115962.
[17] E. Muchuweni, T.S. Sathiaraj, H. Nyakotyo, Effect of gallium doping on the structural, optical and electrical properties of zinc oxide thin films prepared by spray pyrolysis, Ceram. Int. 42 (2016) 10066.
[18] M. Fadel, I.S. Yahia, G.B. Sakr, F. Yakuphanoglu, S.S. Shenouda, Structure, optical spectroscopy and dispersion parameters of $ZnGa_2Se_4$ thin films at different annealing temperatures, Optic Commun. 285 (2012) 3154.
[19] N.F. Mott, E.A. Davis, Electronic Process in Non-crystalline Materials, Calendron Press, 1979 Oxford.
[20] G. Bakiyaraj, J.B.M. Krishna, G.S. Taki, K. Selvaraju, R. Danasekaran, 45 keV N5+ ions induced spikes on CdS thin films: morphological, structural and optical properties, Appl. Surf. Sci. 449 (2018) 233–238.
[21] F. Hanini, A. Bouabellou, Y. Bouachiba, F. Kermiche, A. Taabouche, M. Hemissi, D. Lakhdari, Structural, optical and electrical properties of $TiO_2$ thin films synthesized by sol–gel technique, IOSR J. Eng. 3 (2013) 21.
[22] Guang-lei Tian, He Hong-Bo, Jian-Da Shao, Effect of microstructure of TiO2 thin films on optical band gap energy, Chin. Phys. Lett. 22 (2005) 1787.
[23] J.A. Borrego Pérez, Maykel Courel, Mou Pal, F. Paraguay Delgado, N.R. Mathews, Effect of ytterbium doping concentration on structural, optical and photocatalytic properties of TiO2 thin films, Ceram. Int. 43 (2017) 15777.
[24] N.K. Divya, P.P. Pradyumnan, Photoluminescence quenching and photocatalytic enhancement of Pr-doped ZnO nanocrystals, Bull. Mater. Sci. 40 (2017) 1405.
[25] W. Bai, W.F. Xu, J. Wu, J.Y. Zhu, G. Chen, J. Yang, T. Lin, X.J. Meng, X.D. Tang, J.H. Chu, Investigations on electrical, magnetic and optical behaviors of five-layered Aurivillius Bi6Ti3Fe2O18 polycrystalline films, Thin Solid Films 525 (2012)

195.
[26] J. Yang, Y. Hu, C. Jin, L. Zhuge, X. Wu, Structural and optical properties of Er-doped TiO2 thin films prepared by dual-frequency magnetron co-sputtering, Thin Solid Films 637 (2017) 9.
[27] B. Choudhury, A. Choudhury, Oxygen defect dependent variation of band gap, Urbach energy and luminescence property of anatase, anatase–rutile mixed phase and of rutile phases of TiO2 nanoparticles, Physica E 56 (2014) 364.
[28] J.-P. Lee, J.S. Jang, H. Rhu, H. Yu, B.Y. You, C.S. Kim, K.J. Kim, Y.J. Cho, S. Baik, W. Lee, In situ control of oxygen vacancies in $TiO_2$ by atomic layer deposition for resistive switching devices, Nanotechnology 24 (2013) 295202.
[29] M.N. Huang, Y.Y. Ma, X.Y. Huang, S. Ye, Q.Y. Zhang, The luminescence properties of Bi3+ sensitized Gd2MoO6:RE3+ (RE=Eu or Sm) phosphors for solar spectral conversion, Spectrochim. Acta, Part A 115 (2013) 767.